GREEN AQUA-OXO-HYDROXYLATED ADVANCED MATERIAL FOR TREATMENT OF LIQUID WASTE WITH COMPLEX CONTAMINATION

Ovidiu-Dorin ALUPEI-COJOCARIU[1], Alexandra BANU[2], Manuela Roxana DIJMĂRESCU[3], Dragoş-Ştefan PREDA[4], Elena RUSU[5], Petrişor-Zamora IORDACHE[6]

An aqua-oxo-hydroxylated advanced material was fabricated and directed for the treatment of liquid waste with complex contamination, and particularly for treatment of leachate. The material is capable of removing in one step most contaminants irrespective of contaminants type and contamination charge of leachate. The treatment solution we examined led to a significant reduction in the contamination level of the treated leachate. Specifically, the total nitrogen decreased from 5620 mg/L to 42 mg/L, the biochemical oxygen demand decreased from 3121 mg O_2/L to 42 mg O_2/L, and the chemical oxygen demand decreased from 25571.2 mg O_2/L to 160 mg O_2/L.

Keywords: leachate, waste, liquid waste, wastewater treatment, waste treatment technologies, sludge, chemical inactivation, waste disposal

1. Introduction

In general, liquid waste means an aqueous stream that collects various types of chemical and biological impurities (i.e. contaminants) that exceed the concentration limits allowed by regulatory authorities and that must be removed by a treatment process. The most common liquid wastes are, for example, wastewater [1], industrial wastewater and sludge generated by industrial processes [2], contaminated water from manufacturing processes and post-treatment sludge [3], including various types of organic and inorganic contaminants that may be soluble

[1] Assoc. Prof., Dept. of Manufacturing Engineering, National University for Science and Technology POLITEHNICA Bucharest, Romania, e-mail: ovidiu.alupei@gmail.com
[2] Prof., Dept. of Manufacturing Engineering, National University for Science and Technology POLITEHNICA Bucharest, Romania, e-mail: alexandrabanu14@yahoo.com
[3] Eng., National University for Science and Technology POLITEHNICA Bucharest, Romania, e-mail: manuela-d@live.com
[4] Eng., GREEN WATERNANOTECHNOLOGY, Bucharest, Romania, e-mail: darck.ro14@gmail.com
[5] Eng., GREEN WATERNANOTECHNOLOGY, Bucharest, Romania, e-mail: office@greenwaternanotechnology.ro
[6] Phys., GREEN WATERNANOTECHNOLOGY, Bucharest, Romania, e-mail: iordachezamora1978@gmail.com

or insoluble [4]. Typically, each liquid waste released by discrete contamination sources has one unique footprint of the contamination charge which is marked by the type and amount of each contaminant forming the charge [5,6]. Therefore, this is one of the main reasons the treatment of each waste stream demands technical solutions particularly adapted to remove each specific contaminant making the contamination charge [7].

Although liquid waste gives rise to many thorny problems with environmental profound implications therefore promoting the shaping of the entire socio-economic climate, the technical regulations realize only indistinctive classifications wherein the above-mentioned waste are sorted as hazardous and non-hazardous liquid waste without considering other further relevant evidence in connection to chemical behavior and further fate of each individual contaminant present in the influent waste streams [8,9]. In addition to those above, the regulatory authorities impose clear discharging limits only for certain types of contaminants, whereas the other contaminants are regulated by recording some exhaustive water quality parameters that cumulate the contribution of many different sorts of contaminants, such, as for example, non-regulated soluble organic contaminants [10,11]. The evidence presented by the scientific community undoubtedly proves that some of contaminants not specifically regulated may be very toxic, but in spite of that they are further on released into surface waters streams where they are randomly assimilated by environment components thus affecting on long-term, through cascaded effects, the physical, chemical, and biological attributes of the biota on which, in the end, irreversibly degrade them [12,13].

The most significant drawbacks of current solutions in liquid waste treatment are the limitation in contaminant removal efficiency and waste treatment costs, wherein, in most treatment applications, typically several of current solutions are used to solve one single particular type of liquid waste [14]. Even under such circumstances, the existing treatment solutions give rise to soluble degradation byproducts that further impurity the streams of clean treated water which to be solved requires other additional expensive investments and equipment. It goes without saying that the current treatment chemicals, even if they are used discreetly or combined in different treatment steps, they are the main component responsible for the generation of soluble byproducts as a result of discrete chemical interaction with each individual contaminant, and therefore, the solving of the process for treating the liquid waste is difficult to be realized since is strongly related to the amount and diversity of contaminants loading the influent liquid waste stream [15,16]. In the context herein, finding solutions to solve drawbacks associated with the separation of contaminants from the liquid waste comprising various sorts of contaminants is an urgent priority, but the separation of persistent contaminants and toxic ones which may induce toxicity effects through bioaccumulation is even a more pressing priority [17].

In spite of many technological advances, the main drawbacks of leachate treatment solutions currently in operation are well known wherein, combined solutions attains up to 95% BOD and 50% nitrogen removal efficiency when used in combination with sequencing batch reactors; the membranes filtration brings operational flexibility but also, high operational costs, and high energy consumption; the up-flow anaerobic sludge blanket is economical but has very low efficiency and is highly restrictive in operation due to ammonia toxicity from leachate; the activated sludge is capable of reaching removal efficiencies of about 90% of BOD, 99% of COD, and 80–99% of metals, but also has high operational costs, low efficiency in bacteria removal, and removal efficiency sensible to waste toxicity; sequencing batch reactor may reach removal efficiencies up to 76% of COD, 84% of BOD, and 65% ammonia nitrogen, but typically the influent ammonia affects the COD removal rate; the trickling filters may remove up to 75% ammonia nitrogen but are less effective in solving liquid waste with high organic content; Advanced Oxidation Process typically used to partially remove recalcitrant contamination but require high operational costs and is difficult to bring and maintain in operation treatment process; the coagulation and flocculation are effective in removing organic matter and heavy metals but are very expensive solutions and generates large amounts of chemical sludge; hybrid solutions are more effective and economical compared to individual methods, but not all combinations are feasible [18]. Many works using metal oxides and metal oxide-based nanocomposites were reported in the literature, such us, for example, MgO, TiO_2, MnO_2, Fe_3O_4/Fe_2O_3, CuO/Cu_2O, MnO_2, Al_2O_3, Ag_2O, ZnO, and the like wherein, particular attention was brought to the catalytic, electrochemical, and electro-oxidation applications mainly directed to remove organics and heavy metals [19,20]; few such applications are known that revealing their main limiting drawbacks, which are the price, limited removal efficiency and its sensitivity towards liquid waste composition and toxicity, and the occurrence of various soluble toxic treatment byproducts [21]. Compared to the above-said existing solutions, this work investigates a paradigm shift in liquid waste treatment by proposing a new treatment solution that uses preformed complex mixtures of cationic oxides and hydroxides and hydrated forms thereof, whose chemical activity depends on pH and is capable of giving rise to various ligand exchange and chemical condensation reactions both by interacting each other and with waste contaminants, wherein the result of such transformations is directed to formation of insoluble condensed compounds and water. As will be appreciated herein, the use of such oxyanionic mixtures as process chemicals for the treatment of liquid waste may be a viable option to already existing treatment solutions, wherein its major benefits are brought by removal in one step of most contaminants, high removal efficiency, low treatment costs, its ability to avoid the release of contaminant byproducts during treatment. The second part of this work separately presents the

main findings gained when the after-treatment sludge (i.e. sludge after treating liquid waste) underwent a thermolysis process for its chemical inactivation.

2. Experimental

2.1. Preparing the aquo-hydroxylated admixture

The preparation of the material we used herein (the aquo-hydroxylated mixture, "the material") was made within a 5 liters (i.e. 5 L) mixer with jacket heating wherein, the starting intermediary composition for processing was made by admixing Fe_2O_3 (0.8 kg), Al_2O_3 (0.4 kg), CaO (0.1 kg), MgO (0.1 kg), Mn_2O_3 (0.1 kg), TiO_2 (0.2 kg), P_2O_5 (0.1 kg), and 2 L water. Successively was adding 0.5 L of aqueous H_2O_2 solution (concentration of about 30 wt. %), 0.5 L of aqueous H_2SO_4 solution (concentration of about 50 wt. %), 0.25 L of aqueous H_3PO_4 solution (concentration of about 50 wt. %), and 0.4 L of aqueous HCl solution (concentration of about 37 wt. %) and hence, the pH of the admixture before undergoing further chemical processing was adjusted to about 4. Further on, the mixture was homogenized for 4 hours at 80^OC and 8 RPM.

In a discreet step (2), to the batch already preformed as above were added $Fe(OH)_2$ (0.1 kg), $Al(OH)_3$ (0.2 kg), $Ca(OH)_2$ (0.2 kg), $Mg(OH)_2$ (0.2 kg), and 0.6 L of aqueous sodium silicate solution (concentration of about 40 wt. %), hence forming an intermediary admixture wherein the pH was about 7.3. The mixture undergoing step (2) was mixed for three hours at 80^OC and 8 RPM. Next, to the admixture formed in step (2), as above, was added about 0.85 L of aqueous NaOH solution (concentration of about 50 wt. %), therefore pH was raised to about 11; further on, the chemical condensation mixture was mixed for another two hours at 80^OC and 8 RPM. In further, the process of forming the material composition was stopped, and the material composition was maturated for 24 hours to obtain the finished material. All chemicals used were procured from Merck, among which Fe_2O_3 powder (<5 μm particle size, ≥96%), Al_2O_3 powder ultra dry (0.063-2 mm particle size), MgO nanopowder (≤50 nm particle size).

In the other discreet step (3), the excess water was removed from the maturated material composition until the moisture content reached 25 wt. % (16-40 μm borosilicate sieve); in the next forming step, the dewatered cake was dried at 90^OC until the moisture content reached 10 wt. % (Memmert UF450plus oven), then dried material was milled and transformed into a fine powder with a grinding size of less than 1 mm (GRINDOMIX GM 200). 2.75 kg of powdered finished composite material was made. Finally, the material was finished by adding 0.4 kg of ground kraft paper (fiber sizes less than 0.5 mm), and the resulting composition was blended for another two hours.

2.2. The leachate

The leachate sampled from a waste deposit was treated with the material formulation prepared as above to separate water from contaminants (as described in more detail below in section 2.3); the formulated material was used as a waste treatment chemical. After finishing the leachate treatment, the water was separated from the impurifying solid suspensions, hence resulting in the treated water and after-treatment sludge.

2.3. The leachate treatment

A total of three equivalent evaluation batches (pilot studies) were made. The leachate was treated by using a dosing rate of 50 g per liter to form the treatment admixture, wherein the total volume of the treatment admixture batch was about 20 L of leachate. After adding the material, the pH of the treatment admixture was raised to 10 by using NaOH, and then the mixture was homogenized for 4 hours at a constant mixed rate of 10 RPM (IKA Electronic overhead stirrer). Next, the pH was adjusted to 8.5 with $FeCl_3$ (concentration of about 40 wt. %), and then to 7.5 with aluminum polychloride solution (concentration of about 30 wt. %). Formed solid suspensions were separated from the treatment admixture by filtration (Cytiva Whatman™ Grade 597 paper sheet), wherein the filter retention size was from 4 to 7 μm. Treated levigate obtained after filtration (clean water after flocs separation) was sampled and sent to be investigated by a licensed environmental laboratory with the aim of treatment quality assessment: the results are shown in Table 1. Additionally, separated aqueous sludge was placed for another 72 hours on a porous glass fiber membrane (0.45 μm) wherein at the end were obtained 5.2 kg of dewatered sludge (water content of about 68 wt. %).

2.4. Analytical investigations

Morphostructural investigations were performed by transmission electron microscopy using a Philips S208 electronic microscope. Morphochemical investigations were made by scanning electron microscopy using combined a VEGA III microscope, whereas the microanalysis investigations were performed using a QUANTAX 400 X-ray spectrometer. The spectrometric investigations were realized by Fourier-transform infrared spectroscopy using a FTIR-6300 (JASCO) equipment (FTIR) to assess the functional structure of the material, contaminants loading the leachate, and after-treatment sludge.

The levigate before treatment and clean water after treatment were separately investigated through specific analytical procedures as described in more detail below. The contaminant removal efficiency reached 99.25% for total N, 98.65% for BOD, 99.37% for COD, 99.69% for phenols, 98.45% for TSS, 97.91% for solid residue obtained by evaporation at 105°C, and 79.81% for sulfates. This evidence illustrates that the solution we investigated is capable of removing in one

step the majority of contaminants at unprecedented removal efficiency of over 99%, except sulfates. As a whole, we conclude the solution we investigated reached a removal efficiency of about 99% of all organics and about 80% of all inorganic contamination.

Table 1

The concentration of most relevant contaminants measured before and after levigate treatment

Analyte	Results before treatment	Method	Analyte	Results after treatment	Method
total N	5620 [mg/L]	W-NTOT-PHO[1]	total N	B1[6] - 50 [mg/L] B2[7] - 46 [mg/L] B3[8] - 30 [mg/L]	W-NTOT-PHO[1]
(BOD)[2]	3121 [mg O_2/L]	W-BOD5-ELE[1]	(BOD)[2]	B1 - 46 [mg O_2/L] B2 - 36 [mg O_2/L] B3 - 44 [mg O_2/L]	W-BOD5-ELE[1]
(COD)[3]	25571.2 [mg O_2/L]	W-CODCR-PHO[1]	(COD)[3]	B1 - 188 [mg O_2/L] B2 - 140 [mg O_2/L] B3 - 152 [mg O_2/L]	W-CODCR-PHO[1]
phenol index	43.22 [mg/L]	W-MPHI-PHO[1]	phenol index	B1 - 0.162 [mg/L] B2 - 0.192 [mg/L] B3 - 0.045 [mg/L]	W-MPHI-PHO[1]
TSS[4]	776 [mg/L]	W-TSS-GR[1]	TSS[4]	B1 - 16 [mg/L] B2 - 11 [mg/L] B3 - 9 [mg/L]	W-TSS-GR[1]
SRE[5]	59434 [mg/L]	W-TDS-GR-R[1]	SRE[5]	B1 - 1520 [mg/L] B2 - 860 [mg/L] B3 - 1340 [mg/L]	W-TDS-GR-R[1]
Sulfate	104 [mg/L]	W-TDS-GR-R[1]	Sulfate	B1 - 25.9 [mg/L] B2 - 21.5 B3 - 18.6	W-TDS-GR-R[1]

[1]own analytical procedure [2]biochemical oxygen demand [3]chemical oxygen demand [4]total suspended solids
[5]solid residue on evaporation at 105°C [6]batch 1 [7]batch 2 [8]batch 3

3. Experimental

3.1. Advanced material

The material was directed to be made by chemical dissolution at low pH of metal oxides used as starting materials to form soluble aquo-oxo-hydroxylated speciations of Fe, Al, Ca, Mg, Mn, Ti, and P; then chemical condensation of as above preformed soluble admixture at high pH; wherein, in the end the chemically condensed aquo-oxo-hydroxylated speciations are reformed as one unique multicomponent aquo-oxo-hydroxylated material. The condensation process herein results in the forming of a new material which incorporates aquo-oxo-hydroxylated components of Fe, Al, Ca, Mg, Mn, or Ti, such as, for example, cationic oxo-speciations with mixed morphochemical compositions similar to oxysalt minerals.

3.2. Assessment of treatment quality

The material was directed to be made by chemical dissolution at low pH of metal oxides used as starting materials to form soluble aquo-oxo-hydroxylated speciations of Fe, Al, Ca, Mg, Mn, Ti, and P; then chemical condensation of as above preformed soluble admixture at high pH; wherein, in the end the chemically condensed aquo-oxo-hydroxylated speciations are reformed as one unique multicomponent aquo-oxo-hydroxylated material. The condensation process herein results in the forming of a new material which incorporates aquo-oxo-hydroxylated components of Fe, Al, Ca, Mg, Mn, or Ti, such as, for example, cationic oxo-speciations with mixed morphochemical compositions similar to oxysalt minerals.

The leachate compositions are complex mixtures typically comprising soluble and suspended contaminants leached from the solid substrate through they pass (such us, for example, soils and waste deposits) which, among others includes complex chemical compounds such as for example salts, ammonia, heavy metals, humic and fulvic acids, phosphates, organic acids, aldehydes, alcohols, simple sugars, and derivatives thereof [22,23]. The main reason that is difficult to treat this type of liquid waste is it forms highly charged supersaturated solutions that realize complex electrolytic equilibria at high pH; this is one reason why when attempting to lower the pH to break such equilibria, more degradation byproducts are formed which realizes even more complex chemical equilibria. To explain the existence of such chemical equilibria at high pH reasonably may be assumed that mineral and organic compounds leached by water when passing through the soil, wherein, due to their chemical variety, the pressure exerted by the weight of soil layers, and concentration of each component, and hence the composition of leachate may comprise cationic complexes, basic salts, counterions and mixed counter-species of the above, cationic aqua-oxo-hydroxylated complexes, and the like.

Biochemical oxygen demand (BOD) is typically used as an indicator for the concentration of organic matter in water hence expressing the total organic content that is available to microorganisms, plus any other compounds that spontaneously

react with O_2. Chemical oxygen demand (COD) measures all organic matter in a sample that is able to be oxidized to carbon dioxide but does not include the oxygen needed for nitrification.

First, by correlating the measured values of total N, BOD, COD, and SRE shown in Table 1, can be concluded that the total residual suspended solids in clean water are mainly inorganic in nature, and most likely consisting of aquo-oxo-hydroxylated species of Fe, Al, Ca, Mg, Mn, and Ti, such as, for example, hydrated oxides and hydroxides of said cations that exist as particles of a very small size able to pass through filter, or soluble species of the above cations which cannot be further transformed by oxidation. Additionally, the measurement results above are in agreement with the results of the phenol index test in Table 1 which measured a residual amount of about 0.133 mg/L.

Considering that COD indicator does not provide a time frame or the way in which the organic contaminants are actually oxidized in situ, to correlate the COD measurement with the measurement results of the other quality parameters we mentioned above, then we shall naturally assume that potassium dichromate ($K_2Cr_2O_7$) which is reduced during testing under acidic conditions is actually consumed to oxidize the residual cationic aquo-oxo-hydroxylated speciations left in water after treatment. In addition to that above, we suspect that, during the test, $K_2Cr_2O_7$ forms very reactive aquo-oxo-hydroxylated cationic species with chemical behavior similar to that of reactive oxygen species that passed through filter, hence contributing to free oxygen depletion; considering these evidence, is possible BOD and COD are lower than the measurements indicated, and therefore, the level of residual organic matter is possible may be of similar order magnitude to that indicated by the phenol index measurements.

3.3. Morphostructural investigations

The investigations in Fig. 1(a) disclose a clear distinctive morphostructural composition of advanced material, whose sizes dimension discretely ranges from a few nanometers up to 200 hundred nanometers or even more.

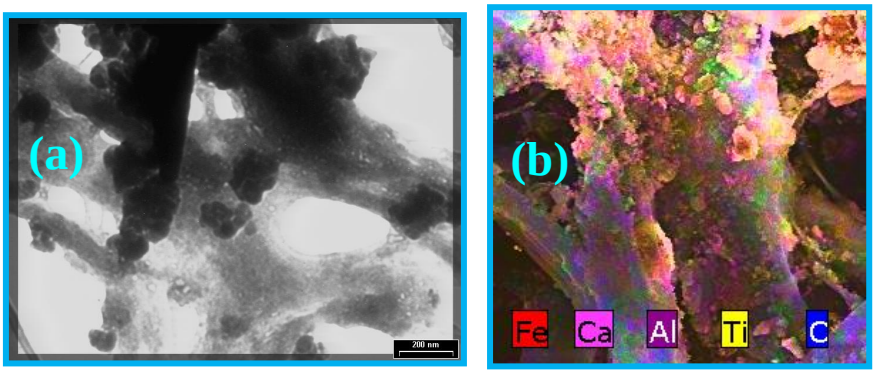

Fig. 1. Morphostructural investigations of finished material (a) TEM micrographs; (b) elemental mapping of finished material

On the contrary, the evidence in Fig. 2 and Fig. 3(a) indicates that the morphostructure of material in dewatered sludge is shapeless.

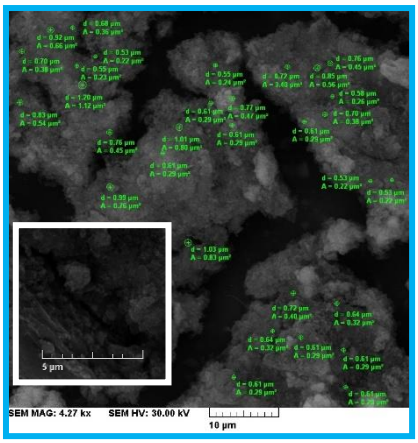

Fig. 2. SEM micrograph of after-treatment dewatered sludge

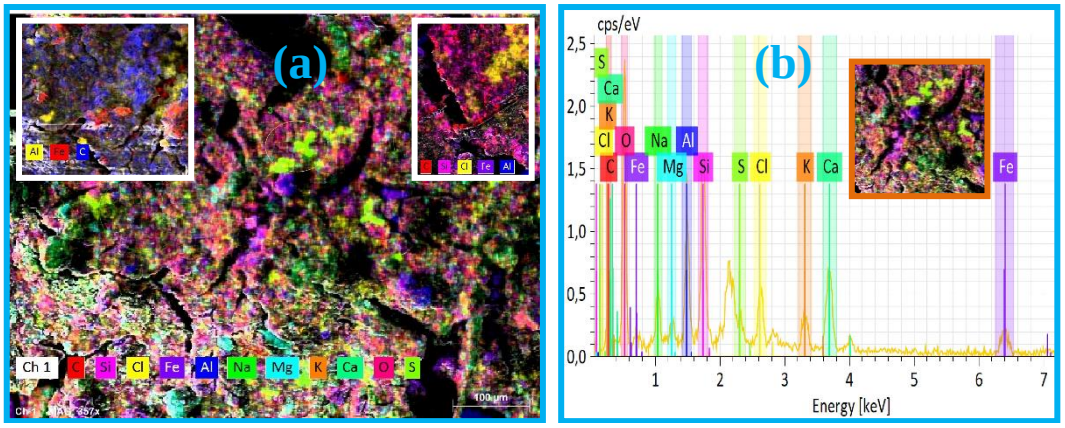

Fig. 3. Dewatered sludge: (a) mapping the chemical elements forming the composition of dewatered sludge (b) the energy-dispersive X-ray spectra associated with elements found on the above map

This evidence indicates the structure of components forming the material is destructured during treatment, and then restructured during pH adjusting, hence forming amorphous compositions incorporating contaminants and other solid impurities not chemically bonded to them. The mass percent of carbon and nitrogen in dewatered sludge rose with an average of over 22.3% and 18.8%, based on the total mass percent amassing all chemical elements measured on the EDX maps.

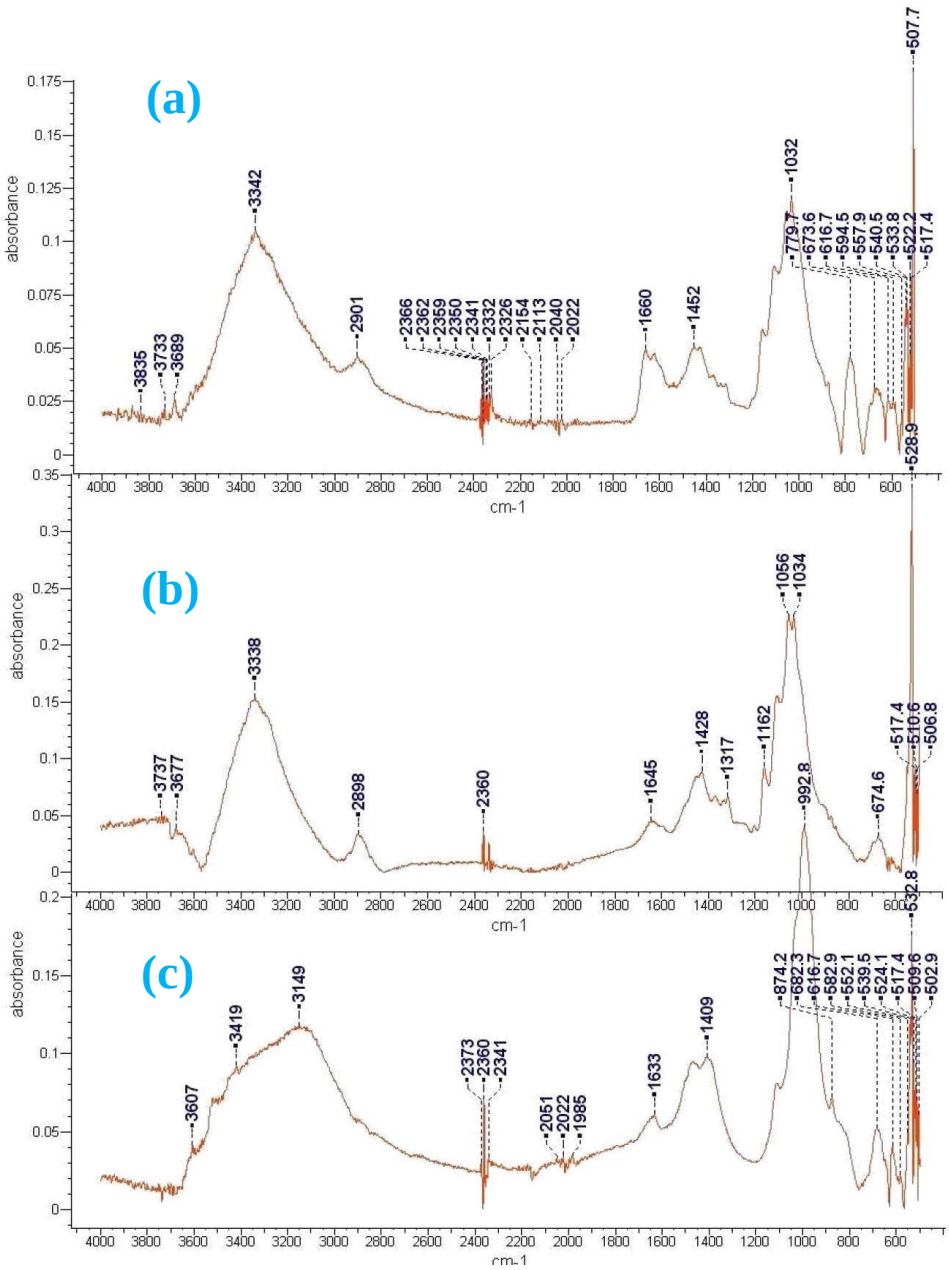

Fig. 4. FTIR investigations of (a) finished advanced material, (b) material charged with contaminants, (c) the dewatered sludge after treating leachate

By analyzing the FTIR spectra of advanced material and of material charged with contaminants can be observed that their spectra profiles mainly keep unchanged their analytical distribution profiles, except their absorption intensity, and spectra region from 500 to 800 cm^{-1}, wherein the structure of peaks before and

after treatment transforms completely. As will be appreciated herein, these evidence indicates the main process for contaminant bonding is the ligand exchange, including among others aquo ligands (H_2O), oxo ligands (=O), and hydroxyls ligands (-OH).

As expected, the IR spectra of leachate in Fig. 4(c) indicate a complex contamination comprising various compounds having various chemical functionalities as described in more detail below. More specifically, the contaminants forming the leachate composition are compounds whose chemical structure incorporates numerous types of chemical functionalities, as follow: the peaks at 3149 cm^{-1} and 3677 cm^{-1} were attributed to $\nu_{as}(NH_4)$ [29, 30]; the water coordinated to metal cations; ν(OH) wherein, typically a broad band around 3200 cm^{-1} and other small bands at 3605 cm^{-1} and 3580 cm^{-1} which are associated with the presence of free acids; the ν(OH) of free hydroxyls around 3300 cm^{-1} [24]. The adsorption profile of broad band between 2300–2400 cm^{-1} comprises several peaks which were attributed to $\nu_3(CO_2)$ and ν(O−H) from phosphonate group (P−OH) at 2360 cm^{-1}; $M^{2+/3+}$−N_2 [36, 37, 38], $\nu_3(CO_2)$, ν(CN), ν(N−N), C−N, and their species at 2334 cm^{-1}.

The adsorption profile in the range from 1000 cm^{-1} to 2100 cm^{-1} is a large broad band with moderate to high absorption intensities wherein only five distinctive peaks were noted at 992.8 cm^{-1}, 1105 cm^{-1}, 1409 cm^{-1}, 1470 cm^{-1}, 1633 cm^{-1} (predominant contaminants). The main peak on the broad band 980 cm^{-1} to 1100 cm^{-1} may be attributed to contaminants comprising =C−H (in plane bend), double M=O bonds, CO, N_2, ν(N−O), bridging sulfates, $\delta_s(NH_3)$ (coordinated ammonia), ν(NH), ν(C−N) [26, 27], C−N vibrations of the imidazole ring, coordinated ammonia, aliphatic C−C stretchings, $\nu_{as}(COO-)$ and $\nu_s(COO-)$ carboxylate [25], C=C modes of the S-substituted benzene ring, ν(C=S), NO_2 (nitrates), C−O modes, ν(CO), ν(C−Cl), ν(O−O), M−O / M−OH, moieties coordinated to M^{3+} sites, P−O, μ_3−OH, anhydrides ν(COC), M^{3+}−O^{2-}, ν(OH) free hydroxyls, ν(S−O), ν(S=O), S−O stretching vibrations, SO_3H, or νas(SO_3) functional groups (sulfation), wherein M is a metal cation. In addition, the main peak on the broad band 1380 cm^{-1} to 1530 cm^{-1} was attributed to contaminants comprising $\nu_2(CO_2)$, $\nu_s(COO^-)$, in-plane deformation of OH in carboxylic acids, $\delta_s(CH)$, NH_3 oxidation, $\delta_s(NH_3)$ coordinated ammonia, nitrito-species, ν(C−C) of the phenylene group, NH^{4+} cations [29, 30], $\delta_{as}(NH_4)$, $\nu_{as}(C-N)$, ν(N−N), NH_2 species, C−H wagging modes, $\nu_s(SO_3^{2-})$ and $\nu_{as}(SO_3^{2-})$, ν(C=C) and ν(C=N), $\nu_{as}(NO_2)$, ν(C=O) [28], ν(C−C) ring stretchings, −C=O−O bonds, and strongly H-bonded hydroxyls. In addition, the main peak on the broadband 1600 cm^{-1} to 1700 cm^{-1} was attributed to contaminants comprising C=C, $\nu_{as}(COO^-)$ and $\nu_s(COO^-)$, aromatic carboxylic acids,−C=O−O bonds, $\nu_{as}(CO)$, ν(CO) band in ketones, ν(C=C), C=C bond in alkenes, aliphatic carboxylic acids, $\nu_{8a}(C=C)$ mode of the benzene ring, C=N, C=O, C−C ring stretchings, δ(HOH), ν_3 or $\nu_{as}(NO_2)$, $\delta(NH_2)$

mode, $\delta_{as}(NH_3)$ and $\delta_s(NH_3)$ modes, $\delta_s(NH_4)$ protonated ammonia, NH_2 species, amide bands, ammonium ions, N−H bending, NO_2, water O-coordinated to OH group and having one/two hydrogen H-bonds to carboxylate, H-bonded water, NO^{3-} species coordinated to a metal site, M−X (X = Cl, Br, CH_3, and NO_2) [24, 36, 37, 38].

Most likely the peak at 874.2 cm^{-1} cumulates the adsorption intensities arriving from M−OH, M=O, M−O, M^{3+}−NO, and M−X speciations (X = Cl, Br) [31], wherein M is a metal cation. Additionally, the main peaks on the broadband 500 cm^{-1} to 720 cm^{-1} were attributed to contaminants comprising: ν_{as}(C−Br), CO_2 adsorption, $\delta_s(COO^-)$, organic functionalities bonded to M^{2+} sites, M−Cl/Br [31], ν(C−S), M−S bond, ν(M−O−M), $\nu(\mu_3$-O−M), δ(MOH) modes (centered at 682.3 cm^{-1}); ν_{as}(C−Br), CO_2 adsorption, $\delta_s(COO^-)$, organic functionalities bonded to M^{2+} sites, M−Cl/Br, ν(C−S), M−S bond, ν(M−O−M), $\nu(\mu_3$-O−M), δ(MOH) modes (centered at 616.7 cm^{-1}); $\nu_2(N_3-)$, δ_{as}(≡C−H) bend, bridging sulfates, $\nu_{as}(M_3O)$, M−O, M−OH, C−S stretching modes, M^{2+}−NO, $\omega(H_2O)$ modes (centered at 616.7 cm−1); β_s(COO−), M−O, benzene ring vibrations, ring δ_{as}(C−C), $\nu_{as}(M_3O)$,(centered at 582.9 cm^{-1}); M−O and ν_{as}(M−OC) (centered at 552.1 cm^{-1}); M−O, M−NO, ρ(COO−), $M-O_{linker}$ mode, M−N modes, γ(M−OH), and S=O deformation mode (suite of peaks on broad band from 500 cm^{-1} to 540 cm^{-1}) [24]. These are other conclusive clues in line with the assumption stating that leachate is a saturated electrolytic solution that was formed by dissolving large amounts of mineral fractions during leaching.

When comparing the adsorption profiles of leachate in Fig. 4(c) with those of not-tested finished advanced material (in Fig. 4(a)) and of leachate sludge before treatment (in Fig. 4(c)), can be noted that the experimental evidence indicates the leachate composition is quite similar to that of advanced material in that this contains significant amounts of inorganic fractions later binding organics from leachate. Hence, can be noted that before leachate treatment, the peak at 779.7 cm^{-1} of not tested material cumulates the adsorption intensities arriving from γ(CH), δ(COO−), M−O, ν(O−O) mode, M−(η_2-O_2), and O−M−O (wherein M is a metal cation from the above) [32, 33, 34, 35], but their footprint complete disappears after treatment, hence suggesting this type of functionalities are responsible for contaminants transformation and bonding. We naturally observe that the two adsorption profiles of not tested finished advanced material (in Fig. 4(a)) and leachate sludge before treatment (in Fig. 4(c)) match the adsorption profile of after-treatment sludge, wherein can be observed major transformations only on the adsorption spectral domains from 3000 cm^{-1} to 3500 cm^{-1} and from 500 cm^{-1} to 750 cm^{-1} corresponding to spectral domain marking the aqua-oxo-hydroxylated functionally of material we tested. The only reasonable explanation matching the experimental evidence herein is that the leachate and material undertake ligand exchange by restructuring their chemical structure. Also, it is noted that cannot be

observed appearing other additional adsorption peaks in the after-treatment sludge, meaning the treatment process doesn't generate other impurifying treatment byproducts.

From the evidence above, we conclude the leachate includes plenty types of various contaminants whose structure incorporates numerous types of chemical functionalities.

3.4. Treatment process

The main aqua-oxo-hydroxylated functionalities of advanced material consistent with the manufacturing process above, are depicted by spectral analysis in Fig. 4(c), and hence they are: the water coordinated to metal cations; ν(OH) (typically the broad band around 3200 cm^{-1} and other small bands at 3605 and 3580 cm^{-1} which are associated with the presence of free acidic cationic sites); the ν(OH) of free hydroxyls around 3300 cm^{-1}; ν(O−H) from the phosphonate group (P−OH) at 2360 cm^{-1}; double M=O bonds, bridging sulfates, M−O/ M−OH, moieties coordinated to M^{3+} sites, P−O, μ_3−OH, M^{3+}−O^{2-}, ν(OH) free hydroxyls, ν(S−O), ν(S=O), S−O stretching vibrations, SO_3H, $\nu_{as}(SO_3)$ (the main peak on the broad band 980 cm^{-1} to 1100 cm^{-1}); $\nu_s(SO_3^{2-})$, $\nu_{as}(SO_3^{2-})$, and strongly H-bonded hydroxyls (the main peak on the broad band 1380 cm^{-1} to 1530 cm^{-1}); M−OH, M=O, M−O (the peak at 874.2 cm^{-1}); (the main peaks on the broadband 500 cm^{-1} to 720 cm^{-1}) M−S bond, ν(M−O−M), ν(μ_3-O−M), δ(MOH) modes (centered at 682.3 cm^{-1}); ν(M−O−M), ν(μ_3-O−M), δ(MOH) modes (centered at 616.7 cm^{-1}); bridging sulfates, $\nu_{as}(M_3O)$, M−O, M−OH, ω(H_2O) modes (centered at 616.7 cm−1); M−O, $\nu_{as}(M_3O)$,(peak centered at 582.9 cm^{-1}); M−O (peak centered at 552.1 cm^{-1}); M−O, M−O_{linker} mode, γ(M−OH), and S=O deformation mode (suite of peaks on broad band from 500 $cm^{-1}$to 540 cm^{-1}).

After analyzing the evidence herein, it was concluded that the treatment pH acts as a trigger component which transforms chemically unreactive contaminants into more reactive species which may be bonded, or are bonding, or may be coordinated to metals M. For a certain intermediate pH value in between the leachate pH and the end point of regeneration pH, the treatment mixture continuously undergoes cascaded chain transformations, wherein, the random ligand exchange continues until all reactive functional groups of the contaminants throughout the treatment mixture reach the chemical potential equalization in such equilibrium intermediate state. When the end point of regeneration pH is reached, most of contaminant speciations are transformed into insoluble compounds which can be removed by sedimentation.

4. Conclusions

An aqua-oxo-hydroxylated advanced material was fabricated and directed for the treatment of liquid waste with complex contamination. The advanced

material was tested on a leachate, and extensively investigated by electron microscopy, infrared spectroscopy, and specific lab investigations to assess the quality of treatment and contaminant removal effectiveness. The contaminant removal efficiency reached 99.25% for total N, 98.65% for BOD, 99.37% for COD, 99.69% for phenols, 98.45% for TSS, 97.91% for solid residue obtained by evaporation at 105°C, and 79.81% for sulfates.

Acknowledgements

Work made with government support under Grant number SMIS119960 awarded by the Romanian European Investments and Projects Ministry.

R E F E R E N C E S

[1]. *K. K. Kesari, R. Soni, Q. M. S. Jamal, P. Tripathi, J. A. Lal, N. K. Jha, M. H. Siddiqui, P. Kumar, V. Tripathi, and J. Ruokolainen*,"Wastewater Treatment and Reuse: a Review of its Applications and Health Implications", in Water Air Soil Pollut., **vol. 232**, no. 5, May 2021.

[2]. *M. Ahmed, M. O. Mavukkandy, A. Giwa, M. Elektorowicz, E. Katsou, O. Khelifi, V. Naddeo, and S. W. Hasan*," Recent developments in hazardous pollutants removal from wastewater and water reuse within a circular economy", in npj Clean Water, **vol. 5**, 12, 12 April 2022.

[3]. *Q. Xu, G. Siracuza, S. D. Gregorio, and Q. Yuan,* "COD removal from biologically stabilized landfill leachate using Advanced Oxidation Processes (AOPs)", in Process Saf. Environ. Prot., **vol. 120**, Nov. 2018, pp. 197-210.

[4]. *S. Bonetta, C. Pignata, E.a Gasparro, L. Richiardi, S. Bonetta, and E. Carraro,* "Impact of wastewater treatment plants on microbiological contamination for evaluating the risks of wastewater reuse", in Environ. Sci. Eur., **vol. 34**, 20, March 2022.

[5]. *R. Fuentes, M. Molinos-Senante, F. H. Sancho, and R. Sala-Garrido,* "Analysing the efficiency of wastewater treatment plants: The problem of the definition of desirable outputs and its solution", in J. Clean. Prod., **vol. 267**, 121989, September 2020.

[6]. *R. Mailler, J. Gasperi, G. Chebbo, and V. Rocher,* "Priority and emerging pollutants in sewage sludge and fate during sludge treatment", in Waste Manag Res., **vol. 34**, no. 7, July 2014, pp. 1217-1226.

[7]. *R R. O. Abdel Rahman, H. A. Ibrahium, and Y.-T. Hung,* "Liquid Radioactive Wastes Treatment: A Review", in Water, **vol. 3**, no. 2, May 2011, pp. 551-565.

[8]. *Debra R. Reinhart.,* "A Review Of Recent Studies On The Sources Of Hazardous Compounds Emitted From Solid Waste Landfills: A U.S. Experience", in Waste Manag. Res., **vol. 11**, no. 3, June 1993, pp. 257-268.

[9]. *A. Kumar, A. K. Thakur, G. K. Gaurav, J. J. Klemeš, V. K.Sandhwar, K. K. Pant, and R. Kumar,* "A critical review on sustainable hazardous waste management strategies: a step towards a circular economy", in Environ. Sci. Pollut. Res., **vol. 30**, 105030-105055, Sept. 2023.

[10]. *M. Preisner, E. Neverova-Dziopak, and Z. Kowalewski,* "An Analytical Review of Different Approaches to Wastewater Discharge Standards with Particular Emphasis on Nutrients", in Environ. Manage., **vol. 66**, Sept. 2020, pp. 694-708.

[11]. *M. F. Jaramillo, and I. Restrepo,* "Wastewater Reuse in Agriculture: A Review about Its Limitations and Benefits", in Sustainability, **vol. 9**, 10, Oct. 2017.

[12]. *C. Chen, and K. Xia,* "Fate of Land Applied Emerging Organic Contaminants in Waste Materials", in Curr. Pollution. Rep., **vol. 3**, Feb. 2017, pp. 38-54.

[13]. *M. Wilson, and M. A. Ashraf,* "Fate of Land Applied Emerging Organic Contaminants in Waste Materials", in Environmental Contaminants Reviews, **vol. 1**, June 2018, pp. 01-12.

[14]. *R. Rashid, I. Shafiq, P. Akhter, M. J. Iqbal, and M. Hussain,* "A state-of-the-art review on wastewater treatment techniques: the effectiveness of adsorption method", in Environ. Sci. Pollut. Res., **vol. 28**, Jan. 2021, pp. 9050–9066.

[15]. *K. Sathya, K. Nagarajan, G. C. G. Malar, S. Rajalakshmi, and P. R. Lakshmi*, "A comprehensive review on comparison among effluent treatment methods and modern methods of treatment of industrial wastewater effluent from different sources", in Appl. Water Sci., **vol. 12**, 20, March 2022.

[16]. *L. A. Schaider, K. M. Rodgers, and R. A. Rudel,* "Review of Organic Wastewater Compound Concentrations and Removal in Onsite Wastewater Treatment Systems", in Environ. Sci. Technol., **vol. 51**, 13, June 2017, pp. 7304-7317.

[17]. *B. Sun, Q. Li, M. Zheng, G. Su, S. Lin, M. Wu, C. Li, Q. Wang, Y. Tao, L. Dai, Y. Qin, and B. Meng,* "Recent advances in the removal of persistent organic pollutants (POPs) using multifunctional materials:a review", in Environ. Pollut., **vol. 265**, A, Oct. 2020, pp. 114908.

[18]. *A. Nath, and A. Debnath,* "A short review on landfill leachate treatment technologies", in Mater. Today: Proc., **vol. 67**, 8, Oct. 2022, pp. 1290-1297.

[19]. *T. Naseem, and T. Durrani,* "The role of some important metal oxide nanoparticles for wastewater and antibacterial applications: A review", in J. Environ. Chem. Ecotoxicol., **vol. 3**, Feb. 2021, pp. 59–75.

[20]. *S. Y. Guvenc, Y. Daniser, E. Can-Güven, G. Varank, and A. Demir,* "Pre-coagulated landfill leachate treatment by Electro-oxidation using MMO/Ti, Pt/Ti, and graphite anodes", in Environ. Eng. Res., **vol. 28**, 1, Jan. 2022, 210419.

[21]. *O. Garcia-Rodriguez, E. Mousset, H. Olvera-Vargas, and O. Lefebvre,* "Electrochemical treatment of highly concentrated wastewater: A review of experimental and modeling approaches from lab- to full-scale", in Crit. Rev. Environ. Sci. Technol., **vol. 55**, 2, Sep. 2020, pp. 240-309.

[22]. *R.B. Brennan, E. Clifford, C. Devroedt, L. Morrison, and M.G. Healy,* "Treatment of landfill leachate in municipal wastewater treatment plants and impacts on effluent ammonium concentrations", in J. Environ. Manage., **vol. 188**, March 2017, pp. 64-72.

[23]. *Y. Cherni, L. Elleuch, M. Messaoud, M. Kasmi, A. Chatti, and I. Trabelsi,* "Recent technologies for leachate treatment: a review", in Euro-Mediterr J Environ Integr, **vol. 6**, 79, Dec. 2021.

[24]. *K. I. Hadjiivanov, D. A. Panayotov, M. Y. Mihaylov, E. Z. Ivanova, K. K. Chakarova, S. M. Andonova, and N. L. Drenchev,* "Power of Infrared and Raman Spectroscopies to Characterize Metal-Organic Frameworks and Investigate Their Interaction with Guest Molecules", in Chem. Rev., **vol. 121**, 3, Dec. 2020, pp. 1286-1424.

[25]. *C. Qi, D. Zhang, S. Gao, H. Ma, Y. He, S. Ma, Y. Chen, and X. Yang,* "Crystal Structure and Magnetic Property of a Metal-Organic Framework (MOF) Containing Double-Stranded Chain with Metallomacrocycles and Dinuclear Mn(II) Subunits", in J. Mol. Struct., **vol. 891**, 1-3, Nov. 2008, pp. 357-363.

[26]. *G. C. Shearer, V. Colombo, S. Chavan, E. Albanese, B. Civalleri, A. Maspero, and S. Bordiga,* "Stability vs. Reactivity: Understanding the Adsorption Properties of $Ni_3(BTP)_2$ by Experimental and Computational Methods", in Dalton trans., **vol. 42**, 18, Feb. 2013, 6450-6458.

[27]. *M. Maczka, I. E. Collings, F. F. Leite, and W. Paraguassu,* "Raman and Single-crystal X-ray Diffraction Evidence of Pressure-induced Phase Transitions in a Perovskite-like Framework of $[(C_3H_7)_4N]$-$[Mn(N(CN)_2)_3]$", in Dalton trans., **vol. 48**, 25, May 2019, 9072-9078.

[28]. *P. M. Usov, C. F. Leong, B. Chan, M. Hayashi, H. Kitagawa, J. J. Sutton, K. C. Gordon, I. Hod, O. K. Farha, J. J. Hupp, et al.,* "Probing Charge Transfer Characteristics in a Donor-Acceptor Metal-Organic Framework by Raman Spectroelectrochemistry and Pressure-Dependence Studies", in Phys. Chem. Chem. Phys., **vol. 20**, 40, Sep. 2018, 25772-25779.

[29]. *M. Maczka, P. Kadłubański, P. T. C. Freire, B. Macalik, W. Paraguassu, K. Hermanowicz, and J. Hanuza*, "Temperature- and Pressure-Induced Phase Transitions in the Metal Formate Framework of $[ND_4][Zn(DCOO)_3]$ and $[NH_4][Zn(HCOO)_3]$", in Inorg. Chem., **vol. 53**, 18, Aug. 2014, 9615-9624.

[30]. *M. Maczka, A. Pietraszko, B. Macalik, and K. Hermanowicz*, "Structure, Phonon Properties, and Order-Disorder Transition in the Metal Formate Framework of $[NH_4][Mg(HCOO)_3]$", in Inorg. Chem., **vol. 53**, 2, Jan. 2014, 787-794.

[31]. *M. Díaz-García, M. Sánchez-Sánchez,* "Synthesis and Characterization of a New Cd-Based Metal-Organic Framework Isostructural with MOF-74/CPO-27 Materials", in Microporous Mesoporous Mater., **vol. 190**, 15, May 2014, 248-254.

[32]. *H. Leclerc, A. Vimont, J.-C. Lavalley, M. Daturi, A. D. Wiersum, P. L. Llwellyn, P. Horcajada, G. Férey, and C. Serre*, "Infrared Study of the Influence of Reducible Iron(III) Metal Sites on the Adsorption of CO, CO_2, Propane, Propene and Propyne in the Mesoporous Metal-Organic Framework MIL-100", in Phys. Chem. Chem. Phys., **vol. 13**, 24, May 2011, 11748-11756.

[33]. *V. H. Nguyen, T. D. Nguyen, L. G. Bach, T. Hoang, Q. T. P. Bui, L. D. Tran, C. V. Nguyen, D. N. Vo, and S. T. Do*, "Effective Photocatalytic Activity of Mixed Ni/Fe-Base Metal-Organic Framework under a Compact Fluorescent Daylight Lamp", in Catalysts, **vol. 8**, 11, Oct. 2018, pp. 487.

[34]. *S. Naeimi, and H. Faghihian,* "Application of Novel Metal Organic Framework, MIL-53(Fe) and Its Magnetic Hybrid: For Removal of Pharmaceutical Pollutant, Doxycycline from Aqueous Solutions", in Environ. Toxicol. Pharmacol., **vol. 53**, May 2017, pp. 121-132.

[35]. *J. M. Fernández-Morales, L. A. Lozano, E. Castillejos-López, I. Rodríguez-Ramos, A. Guerrero-Ruiz, and J. M. Zamaro,* "Direct Sulfation of a Zr-Based Metal-Organic Framework to Attain Strong Acid Catalysts", in Microporous Mesoporous Mater., **vol. 290**, Dec. 2019, 109686.

[36]. *R. K. Ameta, and M. Singh*, "-NO and -CN directed Metal Organic Ionic Framework used for Concentration Responsive Adsorption of Organic Pollutant, Bovine Serum Albumin and 2,2-Diphenyl-1-Picrylhydrazyl", in Microporous Mesoporous Mater., **vol. 4**, 6, Feb. 2019, 1922-1929.

[37]. *A. Zanon, S. Chaemchuen, B. Mousavi, and F. Verpoort*, "1 Zn-doped ZIF-67 as catalyst for the CO_2 fixation into cyclic carbonates", in J. CO Util., **vol. 20**, July 2017, pp. 282-291.

[38]. *C. Racles, M. F. Zaltariov, M. Iacob, and M. Silion, Avadanei, M.; Bargan, A.,* "Siloxane-Based Metal-Organic Frameworks with Remarkable Catalytic Activity in Mild Environmental Photodegradation of Azo Dyes", in Appl. Catal., **vol. 205**, May 2017, pp. 78-92.